ROYAL SOCIETY
OF CHEMISTRY

COMMUNICATION

Check for updates

Rapid synthesis of ultra-long silver nanowires for high performance transparent electrodes†

Alexandra Madeira,[abd] Dorina T. Papanastasiou, [c] Thierry Toupance, [d] Laurent Servant,[d] Mona Tréguer-Delapierre, [*a] Daniel Bellet [c] and I. A. Goldthorpe [*b]

By using 1,2-propanediol instead of the classic polyol solvent, ethylene glycol, ultra-long silver nanowires are obtained in only 1 h. These nanowires lead to transparent electrodes with a sheet resistance of 5 Ohms per sq at a transparency of 94%, one of the highest figures of merit for nanowire electrodes ever reported.

There is an increasing demand for optoelectronic devices such as displays, solar cells, transparent heaters, sensors, light-emitting diodes (LEDs), paper-like displays and e-skins.[1,2] In order to produce such components, the development of transparent and mechanically flexible electrodes remains a task of major importance.[3] Most of the transparent electrodes reported to date rely on the use of metal oxide semiconductor layers,[4] indium tin oxide (ITO) being the most common. However, the scarcity and brittleness of the latter has prompted the search for indium-free and flexible transparent electrodes.[5] Silver nanowire (AgNW) networks constitute one of the most promising alternatives, particularly for flexible applications.[6] They combine high electrical conductance with excellent optical transparency, and show minimal conductance decrease with bending.[7,8] Furthermore, low temperature processing methods exist that enable conductance and transparency values on plastics that approach those on glass.[9] It is known from the literature that networks made from longer AgNWs achieve the highly desirable goal of being more conductive at a given transparency.[10] This is because, for a given areal coverage, longer NWs overlap more than shorter NWs, decreasing the extent of NW dead ends not connected into the network.[11]

Furthermore, percolation can be reached at lower areal coverage. The critical density n_c for stick percolation threshold has been shown by Monte Carlo simulations to be $5.64/L_{NW}^2$ where in this application L_{NW} is the NW length.[12] With less NWs required for a connected network, very high transparencies, with the added benefit of lower haze, can be achieved which is useful for applications like displays, touch screens, transparent heaters and smart windows.[12,13] To this end, many groups have sought how to synthesize ultra-long AgNWs,[14,15] which we define as NWs with aspect ratios $\geq$ 1000 and lengths $\geq$ 100 μm. Diameters greater than 50 nm are also desirable to ensure good electrical conductance of the network.[16] Due to its low cost, ease, and ability to produce quality NWs in large volumes, the polyol method is currently the most common method for AgNW synthesis.[14,15] It is thus the preferred method to produce ultra-long ones as well. However, the control of morphological characteristics remains a challenging task. Several groups have shown that introducing traces of halide salts or various organic or inorganic derivatives (*e.g.* Cu^{+}, Fe^{2+}, benzoin) can lead to ultra-long AgNWs.[15] Other experimental parameters such as temperature, stirring speed and the molecular weight of poly-vinylpyrrolidone (PVP) have also been successfully tuned to achieve ultra-long AgNWs.[17] Table 1 lists the characteristics of ultra-long AgNWs achieved by a polyol approach reported in recent years with the temperatures and reaction times used to reach these high lengths. In all cases, either the reaction time required is long or the reaction temperature is relatively elevated to accelerate NW growth rates. Note that some strategies require microwave irradiation or heating in extreme conditions such as solvothermal heating.[18–20] However, concerns exist with regards to their reproducibility as well as cost-effectiveness. Polyol processes that use conventional heating are thus more desirable for industry.

A parameter that has rarely been explored in the pursuit of ultra-long AgNWs is the nature of the reaction solvent. We have previously found that using 1,2-propanediol in the AgNW polyol process instead of ethylene glycol leads to faster reaction kinetics and allows growth at lower temperatures.[21] Although

aUniv. Bordeaux, CNRS, ICMCB, UMR 5026, 33600 Pessac, France. E-mail: mona.treguer@icmcb.cnrs.fr

bDepartment of Electrical & Computer Engineering and The Waterloo Institute for Nanotechnology, University of Waterloo, Waterloo, ON N2L 3G1, Canada. E-mail: igoldthorpe@uwaterloo.ca

cUniv. Grenoble Alpes, CNRS, Grenoble INP, LMGP, F-38000 Grenoble, France

dUniv. Bordeaux, CNRS, ISM, UMR 5255, 33400 Talence, France

† Electronic supplementary information (ESI) available. See DOI: 10.1039/d0na00392a

Table 1 Selected articles of ultra-long AgNWs achieved through a polyol approach[18–20,24–27]

	Length (μm)	Diameter (nm)	Aspect ratio	T °C	Reaction time (h)
Conventional heating	80–100	50–70	1600	170	0.6 (ref. 24)
	100	40	2500	170	2.5 (ref. 25)
	120	30	4000	170	0.67 (ref. 26)
	123	120	1025	130	3.5 (ref. 27)
Solvothermal heating	220	55	4000	130	8.5 (ref. 18)
	>100	40–85	1600	150	5 (ref. 20)
	100	40	2500	170	2.5 (ref. 19)

growth of AgNWs in 1,2-propanediol has been reported elsewhere,[22,23] these features were not exploited to obtain ultra-long NWs. In this work we use 1,2-propanediol to achieve ultra-long AgNWs whose synthesis procedure, unlike other processes implemented in the literature, simultaneously has the three desirable characteristics for scale-up purposes: short reaction time (1 h), relatively low synthesis temperature (140 °C) and high yield of nanowires *vs.* nanoparticles (86%). Secondly, when these AgNWs are formed into a network, they have a relatively low sheet resistance even before any post-deposition processing such as thermal annealing. Thirdly, we show that rod coating is a better deposition method compared to spray coating for long AgNWs as the latter causes either AgNWs curvature or clogging of the spray nozzle. Combined together, we achieve electrodes with a sheet resistance of 5 Ω sq^{-1} at a transparency of 94% which represents one of the highest figures of merit for silver nanowire electrodes deposited using a scalable deposition process.

The synthesis method is based on typical Ag nanocrystal polyol processes,[15] except for the use of 1,2-propanediol as the solvent rather than ethylene glycol. Unlike some other reports of ultra-long AgNW synthesis, no foreign ions were used. The reaction temperature and time were 140 °C and 1 h, respectively. Experimental details are outlined in the (ESI†). With these experimental conditions, AgNWs with high length and

high aspect ratio (1060) could be obtained in a single step. Fig. 1 shows transmission electron microscopy (TEM) and scanning electron microscopy (SEM) images, as well as morphology statistics of the sample produced, for example, with a silver concentration of 19.6 mM. The NWs were obtained with a yield of nanowires *vs.* nanoparticles of 86%. We found that the length and diameter of AgNWs can be tuned solely through altering the concentration of AgNO$_3$. When the concentration was decreased, for example, to 19.3 mM, both the length and diameter decreased. For a concentration between 19.6 mM and 20.4 mM, both the length and diameter increased. However, for a concentration higher than 20.4 mM, the length decreased, and the diameter increased, resulting in silver nanowires with a lower aspect ratio (characterization of some of these samples are shown in Fig. S1† and the dependence of the average diameter and length on the silver nitrate concentration is displayed in Fig. S2†).

1,2-Propanediol greatly impacts the kinetics of the reduction process associated with metal nanowire formation. Mechanistic studies are in progress in order to elucidate the oxidation reaction of 1,2-propanediol. Despite its higher viscosity ($\eta = 40.4$ *vs.* 16.1 mPa s for ethylene glycol), the reduction rate increases by a factor 5 in comparison to ethylene glycol. Nuclear magnetic resonance (NMR) investigations revealed the formation of intermediate products such as acetone and 2,2,4-trimethyl-dioxolane while no trace of propanal could be detected. Acetone likely arises from the dehydration of 1,2 propanediol, and the 2,2,4-trimethyl-dioxolane then stems from an acetalization reaction between acetone and 1,2-propanediol. The anisotropic growth arises from Ag seeds with a decahedral multiple twinned structure as well as silver halide seeds, and the regioselective functionalization of pyrrolidone moieties. Experimental details and mechanisms are outlined in the ESI (Fig. S3†).

The 130 μm long AgNWs characterized in Fig. 1 were used to fabricate transparent electrodes. They were deposited on glass substrates using two different scalable deposition methods, Mayer rod coating and spray coating, then annealed to sinter the NW junctions. The rod coated electrodes had a sheet resistance of 5.0 ± 0.2 Ω sq^{-1} and a transparency at 550 nm of 93.8 ± 0.5%. The spray coated electrodes had a lower figure of merit, with sheet resistance and transparency values of 4.6 ± 0.4 Ω sq^{-1} and 91.1 ± 1.0%, respectively. The transparencies correspond to the total transmittance (specular plus diffusive) with the substrate contribution subtracted. From the SEM
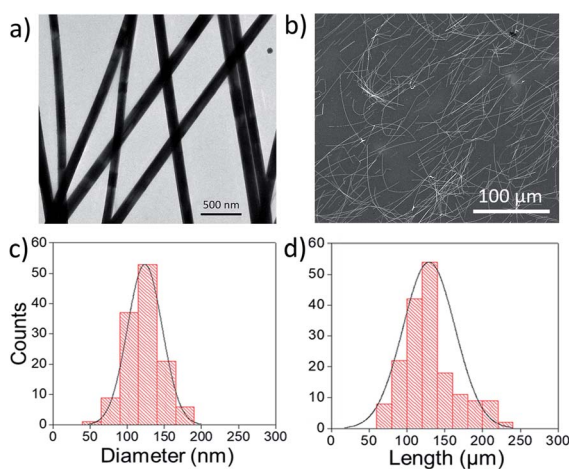

Fig. 1 (a) TEM and (b) SEM images of AgNWs synthesized in 1,2-propanediol with a silver concentration of 19.6 mM. (c) Diameter and (d) length distributions of the sample. The average and distribution values are: $d = 124 \pm 25$ nm and $L = 130 \pm 36$ μm.
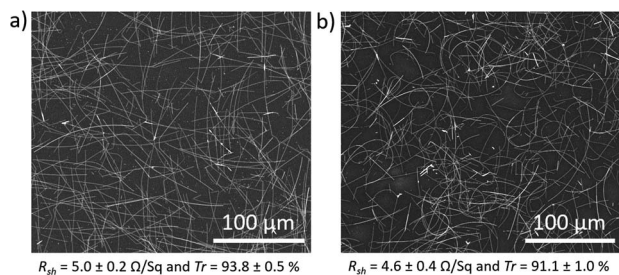
Fig. 2 SEM images of the AgNW networks deposited by (a) Mayer rod coating and (b) spray coating. R_{sh} is the sheet resistance while the stated transmittance (Tr) is at 550 nm and relative to the transmittance of the bare glass.

images of networks deposited by the two methods (Fig. 2 and S4†), it is observed that while both networks are uniform, the spray-coated NWs are curved. The curvature is due to the long length of the NWs which must bend in the droplets that emerge out of the nozzle.[28] On the other hand, the rod-coated NWs are not only more straight, but are somewhat aligned along the 4 orthogonally directed coats.[29] Alignment has been shown in the past to lead to a higher figure of merit.[30]

Interestingly, the sheet resistance of these networks after either deposition method was about 11 Ω sq^{-1} *before* annealing. Typically in other works the resistance of the AgNW network before post-processing treatments (such as thermal annealing, chemical treatments, laser sintering and mechanical pressing) is much higher.[17,31]

The evolution of the resistance *versus* temperature during a thermal ramp of 5 °C min^{-1} in air was tracked in a sample having an initial sheet resistance of 8 Ω sq^{-1} (*i.e.* before any thermal treatment) (Fig. 3). It is compared to the same treatment performed on networks made with commercial AgNWs of similar diameter. Firstly, in stark contrast to the commercial AgNWs, there is little variation in the resistance of our AgNW networks until temperatures above 300 °C. The nanowire junction resistances are decreased somewhat over this range
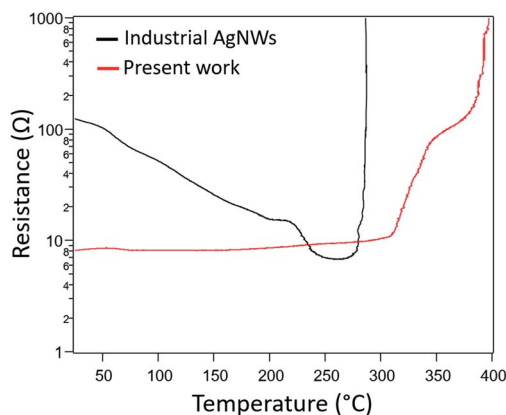
due to sintering, as evidenced by the electrode resistance being lower than its initial resistance when cooled down to room temperature (Fig. S5†). However, an optimized anneal only decreases the as-deposited room temperature sheet resistance by about 55%. Secondly, our AgNWs appear more robust as the dramatic increase of resistance, caused by the spheroidization of the AgNWs (Plateau–Rayleigh instability),[32] does not occur until 320 °C compared to 270 °C for the commercial AgNWs. This spheroidization is shifted even higher to 350 °C when the concentration of AgNWs is decreased (Fig. S6(a)†).

Evidence indicates there are two reasons for the low initial sheet resistance and its minimal reduction *via* thermal annealing: the long NW length, and more importantly, their thin PVP shell. Firstly, networks composed of long nanowires have a lower number of overlapping NW junctions compared to shorter NW networks. Since NW junctions are points of increased resistance, this results in a lower initial sheet resistance. And annealing, which lowers junction resistances, has less of an impact when there are fewer junctions. Regarding PVP, TEM imaging (Fig. S7†) shows that the PVP layer on the surface of our as-synthesized nanowires is very thin, with a thickness less than 0.5 nm. The PVP layer on AgNWs reported by other works is thicker (>1 nm).[33] Our results may be due to a lower ratio of PVP/AgNO$_3$ used compared to other classic polyol processes, as well as the amount of PVP being decreased during the purification step.[34] It has previously been shown that the sheet resistance of unannealed AgNW networks is lower when the PVP shell, an electrical insulator, is thinner.[35] And because the initial junction resistances are lower, these resistances cannot be reduced as much with annealing compared to other works where the PVP shell is typically thicker. Such NWs that do not need any post-deposition treatment to lower sheet resistance would be advantageous for networks used in thermally sensitive applications, such as those deposited on certain polymers or paper, and transparent electrodes deposited on top of organic devices (such as organic solar cells for instance).
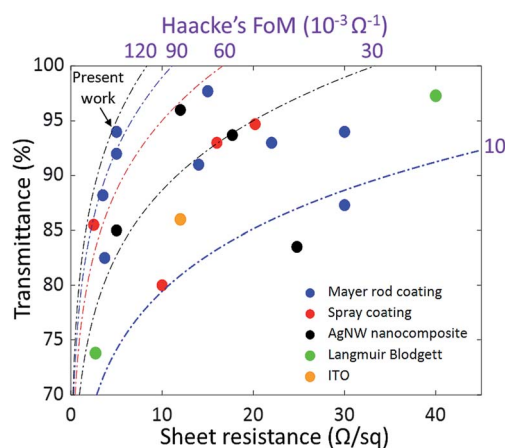

Fig. 3 Temperature evolution of the resistance of electrodes made with industrial AgNWs[16] ($d = 117$ nm and $L = 44$ μm, Seashell Technology, black curve) and with our 130 μm long nanowires (red curve) during a thermal ramp of 5 °C min^{-1} in air.

Fig. 4 Transmittance *versus* sheet resistance of transparent electrodes based on silver nanowires deposited using scalable processes: Mayer rod,[9,19,37,40,42,47,48] spray coating,[24,39,43,45] and Langmuir–Blodgett,[38] as well as AgNW nanocomposites[36,41,44,46] and ITO (ITO purchased from commercial supplier SOLEMS).

In Fig. 4, the transmittance and sheet resistance of our electrodes are compared to other AgNW electrodes in the literature deposited by scalable processes, as well as ITO on glass.[9,19,24,36–48] Iso-values of the Haacke's figure of merit (T_r^{10}/R_{sh}) are also shown. Our electrodes present one of the highest figures of merit of a nanowire electrode in the literature that is deposited using a scalable process. Moreover, it is processed in a very simple way. So far, more sophisticated deposition processes have been used to reach similar performance. For example, Lee *et al.* reported a sheet resistance of 5 Ω sq^{-1} at a transparency of 92% by using a more complicated multi-step post-deposition process involving both mechanical and chemical methods.[42] Other teams reached this performance by using an additional material to make AgNW composites,[39,44,48,49] or by aligning the NWs.[50] By combining such processes with our ultra-long and low-junction-resistance AgNWs, it is expected that higher performance could be reached. Lastly, our nanowires should be easily compatible with the many methods that exist to improve electrode stability and surface roughness such as embedding the NWs in a polymer[36,49,51] and hot-rolling.[9]

In summary, using 1,2-propanediol instead of ethylene glycol as the solvent in the polyol process and selecting the optimal silver concentration in the reaction, we obtained ultra-long AgNWs with an industrially attractive process. Reaction time and temperatures were 1 h and 140 °C, respectively, with no addition of foreign ions. It was found that for our ultra-long NWs, rod-coating leads to better results than spray coating, as the latter imparts curvature into the deposited NWs. We also found that as-deposited NW networks had low sheet resistance without any post-processing such as annealing, an attractive feature for sensitive substrates. Overall, our synthesis and processing methods lead to electrodes with a sheet resistance of 5 Ω sq^{-1} at a transparency of 94%, representing one of the highest figures of merit of all nanowire transparent electrodes deposited using a scalable process. Future work could include exploring the use of 1,2-propanediol in tandem with strategies identified in other studies, such as optimizing temperature and stirring conditions,[24] to obtain even longer AgNWs. And by combining ultra-long NWs with alignment, for example, electrode performance could approach that of metal grids[52] (since there would be few junctions) without the need for lithography. In summary, the easy implementation and scalability of our process exemplify its pertinence as a promising tool towards the development of next generation transparent and flexible electrodes.

Conflicts of interest

There are no conflicts to declare.

Acknowledgements

Notes and references

1 D. Ha, Z. Fang and N. B. Zhitenev, *Adv. Electron. Mater.*, 2018, **4**, 1700593.

2 D. T. Papanastasiou, A. Schultheiss, D. Muñoz-Rojas, C. Celle, A. Carella, J.-P. Simonato and D. Bellet, *Adv. Funct. Mater.*, 2020, **30**, 1910225.

3 W. Cao, J. Li, H. Chen and J. Xue, *J. Photonics Energy*, 2014, **4**, 040990.

4 K. Ellmer, *Nat. Photonics*, 2012, **6**, 809–817.

5 D. S. Hecht, L. Hu and G. Irvin, *Adv. Mater.*, 2011, **23**, 1482–1513.

6 D. Bellet, M. Lagrange, T. Sannicolo, S. Aghazadehchors, V. Nguyen, D. Langley, D. Muñoz-Rojas, C. Jiménez, Y. Bréchet and N. Nguyen, *Materials*, 2017, **10**, 570.

7 A. R. Rathmell and B. J. Wiley, *Adv. Mater.*, 2011, **23**, 4798–4803.

8 V. H. Nguyen, J. Resende, D. T. Papanastasiou, N. Fontanals, C. Jiménez, D. Muñoz-Rojas and D. Bellet, *Nanoscale*, 2019, **11**, 12097–12107.

9 H. Hosseinzadeh Khaligh and I. A. Goldthorpe, *Nanoscale Res. Lett.*, 2014, **9**, 310.

10 M. Marus, A. Hubarevich, R. J. W. Lim, H. Huang, A. Smirnov, H. Wang, W. Fan and X. W. Sun, *Opt. Mater. Express*, 2017, **7**, 1105.

11 S. M. Bergin, Y.-H. Chen, A. R. Rathmell, P. Charbonneau, Z.-Y. Li and B. J. Wiley, *Nanoscale*, 2012, **4**, 1996.

12 D. Langley, M. Lagrange, N. Nguyen and D. Bellet, *Nanoscale Horiz.*, 2018, **3**, 545–550.

13 H. Hosseinzadeh Khaligh, K. Liew, Y. Han, N. M. Abukhdeir and I. A. Goldthorpe, *Sol. Energy Mater. Sol. Cells*, 2015, **132**, 337–341.

14 Z. He, Y. Yang, H. Liang, J. Liu and S. Yu, *Adv. Mater.*, 2019, **31**, 1902807.

15 D. Huo, M. J. Kim, Z. Lyu, Y. Shi, B. J. Wiley and Y. Xia, *Chem. Rev.*, 2019, **119**, 8972–9073.

16 M. Lagrange, D. P. Langley, G. Giusti, C. Jiménez, Y. Bréchet and D. Bellet, *Nanoscale*, 2015, **7**, 17410–17423.

17 L. Sonntag, F. Eichler, N. Weiß, L. Bormann, D. S. Ghosh, J. M. Sonntag, R. Jordan, N. Gaponik, K. Leo and A. Eychmüller, *Phys. Chem. Chem. Phys.*, 2019, **21**, 9036–9043.

18 Y. Zhang, J. Guo, D. Xu, Y. Sun and F. Yan, *ACS Appl. Mater. Interfaces*, 2017, **9**, 25465–25473.

19 Y. Li, X. Yuan, H. Yang, Y. Chao, S. Guo and C. Wang, *Materials*, 2019, **12**, 401.

20 Y. Li, S. Guo, H. Yang, Y. Chao, S. Jiang and C. Wang, *RSC Adv.*, 2018, **8**, 8057–8063.

21 M. Plissonneau, L. Pautrot-D'Alençon, T. Lemercier and M. Tréguer-Delapierre, European Patent No 17306072, 2017, vol. 4, p. 1103.

22 M. R. Johan, N. A. K. Aznan, S. T. Yee, I. H. Ho, S. W. Ooi, N. Darman Singho and F. Aplop, *J. Nanomater.*, 2014, **2014**, 1–7.

23 X. Cong-Wen, Y. Hai-Tao, S. Cheng-Min, L. Zi-An, Z. Huai-Ruo, L. Fei, Y. Tian-Zhong, C. Shu-Tang and G. Hong-Jun, *Chin. Phys.*, 2005, **14**, 2269–2275.

24 L. José Andrés, M. Fe Menéndez, D. Gómez, A. Luisa Martínez, N. Bristow, J. Paul Kettle, A. Menéndez and B. Ruiz, *Nanotechnology*, 2015, **26**, 265201.

25 X. Liu, D. Li, X. Chen, W.-Y. Lai and W. Huang, *ACS Appl. Mater. Interfaces*, 2018, **10**, 32536–32542.

26 Y. Mao, H. Yang, C. Hu, J. Guo, X. Meng and Y. Yang, *J. Mater. Sci. Mater. Electron.*, 2017, **28**, 5308–5314.

27 F. Xu, W. Xu, B. Mao, W. Shen, Y. Yu, R. Tan and W. Song, *J. Colloid Interface Sci.*, 2018, **512**, 208–218.

28 G.-H. Lim, K. Ahn, S. Bok, J. Nam and B. Lim, *Nanoscale*, 2017, **9**, 8938–8944.

29 J. Dong and I. A. Goldthorpe, *Nanotechnology*, 2018, **29**, 045705.

30 S. Kang, T. Kim, S. Cho, Y. Lee, A. Choe, B. Walker, S.-J. Ko, J. Y. Kim and H. Ko, *Nano Lett.*, 2015, **15**, 7933–7942.

31 T. Sannicolo, M. Lagrange, A. Cabos, C. Celle, J.-P. Simonato and D. Bellet, *Small*, 2016, **12**, 6052–6075.

32 D. P. Langley, M. Lagrange, G. Giusti, C. Jiménez, Y. Bréchet, N. D. Nguyen and D. Bellet, *Nanoscale*, 2014, **6**, 13535–13543.

33 L. Sonntag, F. Eichler, N. Weiß, L. Bormann, D. S. Ghosh, J. M. Sonntag, R. Jordan, N. Gaponik, K. Leo and A. Eychmüller, *Phys. Chem. Chem. Phys.*, 2019, **21**, 9036–9043.

34 B. Wiley, Y. Sun and Y. Xia, *Langmuir*, 2005, **21**, 8077–8080.

35 J. Wang, J. Jiu, T. Araki, M. Nogi, T. Sugahara, S. Nagao, H. Koga, P. He and K. Suganuma, *Nano-Micro Lett.*, 2015, **7**, 51–58.

36 A. B. V. K. Kumar, J. Jiang, C. W. Bae, D. M. Seo, L. Piao and S.-H. Kim, *Mater. Res. Bull.*, 2014, **57**, 52–57.

37 H.-G. Cheong, R. E. Triambulo, G.-H. Lee, I.-S. Yi and J.-W. Park, *ACS Appl. Mater. Interfaces*, 2014, **6**, 7846–7855.

38 J.-W. Liu, J.-L. Wang, Z.-H. Wang, W.-R. Huang and S.-H. Yu, *Angew. Chem., Int. Ed.*, 2014, **53**, 13477–13482.

39 F. Selzer, N. Weiß, D. Kneppe, L. Bormann, C. Sachse, N. Gaponik, A. Eychmüller, K. Leo and L. Müller-Meskamp, *Nanoscale*, 2015, **7**, 2777–2783.

40 E.-J. Lee, Y.-H. Kim, D. K. Hwang, W. K. Choi and J.-Y. Kim, *RSC Adv.*, 2016, **6**, 11702–11710.

41 E. Jung, C. Kim, M. Kim, H. Chae, J. H. Cho and S. M. Cho, *Org. Electron.*, 2017, **41**, 190–197.

42 S. J. Lee, Y.-H. Kim, J. K. Kim, H. Baik, J. H. Park, J. Lee, J. Nam, J. H. Park, T.-W. Lee, G.-R. Yi and J. H. Cho, *Nanoscale*, 2014, **6**, 11828–11834.

43 D. Toybou, C. Celle, C. Aude-Garcia, T. Rabilloud and J.-P. Simonato, *Environ. Sci. Nano*, 2019, **6**, 684–694.

44 M. A. Shinde and H. Kim, *Synth. Met.*, 2019, **254**, 97–105.

45 D. Kumar, V. Stoichkov, E. Brousseau, G. C. Smith and J. Kettle, *Nanoscale*, 2019, **11**, 5760–5769.

46 H. Yang, S. Bai, T. Chen, Y. Zhang, H. Wang and X. Guo, *Mater. Res. Express*, 2019, **6**, 086315.

47 Y. Huang, Y. Tian, C. Hang, Y. Liu, S. Wang, M. Qi, H. Zhang and J. Zhao, *ACS Appl. Mater. Interfaces*, 2019, **11**, 21850–21858.

48 Y. Li, X. Yuan, H. Yang, Y. Chao, S. Guo and C. Wang, *J. Mater. Sci. Mater. Electron.*, 2019, **30**, 8883–8891.

49 J. Kim, D. Ouyang, H. Lu, F. Ye, Y. Guo, N. Zhao and W. C. H. Choy, *Adv. Energy Mater.*, 2020, **10**, 1903919.

50 H. Hu, S. Wang, S. Wang, G. Liu, T. Cao and Y. Long, *Adv. Funct. Mater.*, 2019, **29**, 1902922.

51 L. Lian, D. Dong, D. Feng and G. He, *Org. Electron.*, 2017, **49**, 9–18.

52 H. Lu, X. Ren, D. Ouyang and W. C. H. Choy, *Small*, 2018, **14**, 1703140.